



**HAL**  
open science

## **Plasma jet and plasma treated aerosol induced permeation of reconstructed human epidermis**

Vinodini Vijayarangan, Zeineb Maaroufi, Amaury Rouillard, Septuce Zin, Sébastien Dozias, Pablo Escot-Bocanegra, Augusto Stancampiano, Catherine Grillon, Eric Robert

### ► To cite this version:

Vinodini Vijayarangan, Zeineb Maaroufi, Amaury Rouillard, Septuce Zin, Sébastien Dozias, et al.. Plasma jet and plasma treated aerosol induced permeation of reconstructed human epidermis. *Bioelectrochemistry*, 2026, 167, pp.109060. <10.1016/j.bioelechem.2025.109060>. <hal-05202635>

**HAL Id: hal-05202635**

**<https://hal.science/hal-05202635v1>**

Submitted on 7 Aug 2025

**HAL** is a multi-disciplinary open access archive for the deposit and dissemination of scientific research documents, whether they are published or not. The documents may come from teaching and research institutions in France or abroad, or from public or private research centers.

L'archive ouverte pluridisciplinaire **HAL**, est destinée au dépôt et à la diffusion de documents scientifiques de niveau recherche, publiés ou non, émanant des établissements d'enseignement et de recherche français ou étrangers, des laboratoires publics ou privés.



Distributed under a Creative Commons CC BY 4.0 - Attribution - International License

# Plasma jet and plasma treated aerosol induced permeation of reconstructed human epidermis

Vinodini Vijayarangan<sup>a,b</sup>, Zeineb Maaroufi<sup>a,b</sup>, Amaury Rouillard<sup>a</sup>, Septuce Gaetan-Zin<sup>a,b</sup>, Sébastien Dozias<sup>a</sup>, Pablo Escot-Bocanegra<sup>a</sup>, Augusto Stancampiano<sup>a</sup>, Catherine Grillon<sup>b</sup>, Eric Robert<sup>a,\*</sup>

<sup>a</sup> GREMI, UMR7344 CNRS/Université d'Orléans, 14 rue d'Issoudun, BP6744, 45067 Orléans Cedex 2, France

<sup>b</sup> CBM, UPR4301, CNRS Orléans, Rue Charles Sadron, 45071 Orléans, France

---

## A B S T R A C T

---

### Keywords:

Plasma jet  
Plasma treated aerosol  
Skin  
Reconstructed human epidermis  
Permeation  
TEER

As plasma-treated liquids have many applications in plasma medicine, their cutaneous effects for cosmetic purposes are also considered as an alternative way to treat skin without the electric hazards and limitations correlated with the use of a direct plasma. Our previous work on human skin explants showed increased transdermal diffusion of cosmetic ingredients (caffeine, hyaluronic acid) after direct plasma treatment. Despite this proven efficacy, these protocols still face limitations dealing with toxicity, small treatment areas and uneven surface coverage. To overcome these limitations and broaden the scope of non-thermal-plasma-based technology for skin care, this study presents for the first time the development and assessment of a plasma aerosol device to nebulize plasma-treated liquids on skin models.

This work demonstrates how plasma jet and plasma treated aerosol can temporarily enhance permeation in reconstructed human epidermis (RHE), using fluorescein as a probe, under safe plasma delivery conditions. Transepithelial electrical resistance measurements confirm the transient nature of the plasma-induced modulation, suggesting the possibility to control the duration of the enhanced permeation. Overall, the achieved results demonstrate the potential of plasma jet and plasma treated aerosol to safely control diffusion through skin for cosmetic and medical purposes.

---

## 1. Introduction

Cold Atmospheric Plasmas (CAPs) generated with dielectric barrier discharges or plasma jets consist of an ionized gas at atmospheric pressure and operate at nearly room temperature. Because of their unique chemical and physical properties, such as the production of Reactive Oxygen and Nitrogen Species (RONS) and their electric component, CAPs have been developed, assessed and optimized in many fields of applications. Over the past decade, CAPs have been extensively considered and used for numerous biological applications, including clinical protocols and dermocosmetic treatments [1–8]. One key area of interest is enhancing molecular uptake whether in human or murine models, and for both healthy and cancerous cells. The skin's barrier system, while protecting against antigens and harmful substances, also

restricts the penetration of medicines and cosmetics into the skin. Various strategies have been developed to enhance skin absorption, including chemical enhancers and skin ablation devices. However, the high costs and practical limitations of these methods underscore the need for a novel, safe, and accessible approach to improving transdermal delivery. CAPs have been studied to improve cell and tissue permeabilization. Higher uptake of anti-cancer agents by cancer cells [9–11] or an increased penetration of cosmetic ingredients into the skin were demonstrated [1,12–14]. CAPs have previously been shown to be able to interact with human skin in a non-damaging way [1,15,16]. Since European Union regulation forbids animal testing for cosmetic studies, few and selective methods have been developed to allow consistent analysis. Besides quite classical options (i.e. in vitro skin cell culture and in vivo volunteer exposure) two alternatives are nowadays

---

*Abbreviations:* CAP, Cold Atmospheric Plasma; NHEKneo, Normal Human Epidermal Keratinocytes; PBS, Phosphate Buffer Saline; PTA, Plasma Treated Aerosol; RONS, Reactive Oxygen and Nitrogen Species; RHE, Reconstructed Human Epidermis; TEER, Transepithelial Electrical Resistance.

\* Corresponding author.

E-mail address: [eric.robert@univ-orleans.fr](mailto:eric.robert@univ-orleans.fr) (E. Robert).

used in cosmetic studies: human skin explants, as used in our previous study [1] and 3D skin models such as Reconstructed Human Epidermis (RHE).

In our previous study, it was demonstrated that the application of a helium plasma jet on human skin explants can significantly enhance and control the penetration of cosmetic agents such as caffeine and hyaluronic acid [1]. The increase in cosmetic agent penetration was confirmed both by diffusion cells and MS-MALDI techniques while the safety by histological analysis and protein expression. The transient permeation of human explants was demonstrated to be in line with transient modulation of skin features such as surface pH, wettability and transepidermal water loss. All of these parameters were modified right after plasma jet delivery while recovering their baseline value a few minutes (typically 20 min) later. It was demonstrated that this time window also reflected in the transient modulation of the skin barrier. If the solution containing cosmetic agents was applied more than 20 min after the plasma treatment of the human explant no significant variation was observed compared to control.

As reported by Heur et al. [17] also test on volunteer's human skin can provide important information. In their study, Heur and colleagues reported on the skin exposure to a DBD plasma. The skin surface was acidified after 90s of treatment and a relevant increase in microcirculation (up to fourfold) was detected. Fluhr et al. [18] also investigated the effects of a 3-s exposure to an argon CAP jet (Kinpen) on human volunteers. The CAP application led to a decrease in beta-carotene in superficial stratum corneum and an increase of transepidermal water loss indicating an impaired barrier function.

Gelker et al. [19] reported on the exposure of full-thickness human skin and isolated stratum corneum to a DBD plasma. In the study the transepithelial electrical resistance showed a long-term overall drop for treatments  $\geq 90$  s in isolated SC as well as full-thickness skin. Consequently, Franz diffusion cell permeation using differently sized hydrophilic particles enabled an estimation of the pore size and drug transport efficiency. A moderate permeation of particles up to 6  $\mu\text{m}$  in diameter was recorded and attributed to the occasional formation of large pores in the  $\mu\text{m}$ -range. Electroporation was in this case regarded as playing a major role in the enhanced diffusion. The stratum corneum permeabilization for the investigated conditions was shown to be largely irreversible. Choi et al. [20] reported on the effect of a CAP jet on hairless mice to enhance cutaneous delivery, measuring the reduced expression of E-cadherin and reduced intercellular junction formation. This was reported to lead to enhanced absorption of hydrophilic agents, eosin and epidermal growth factor. The reduced skin barrier function was in this case completely recovered within 3 h of exposure to CAP.

The reduced number of works investigating CAP effect on skin is partially due to the limitation imposed by the availability of models. Test on human volunteers and animal models are limited and not always possible while human skin explants are particularly costly, variable in nature and of irregular supply. For these reasons RHEs have been more and more used by many groups for the testing of topical products [21]. While there are several studies on the plasma treatment of human skin cells in vitro (e.g. keratinocytes [22], fibroblasts [23]) the amount of literature on reconstructed human epidermis is scarce.

In one of the few studies, Heuer et al. [17] used a commercial RHE (Episkin) as a skin model to investigate potential harmful effects of plasma treatment. Franz cells were used to measure plasma induced nitric oxide (NO) penetration through epidermis and the measurements highlighted a significant increase following plasma treatment.

In this study, the application of non-thermal plasma jet and plasma treated aerosol (PTA) on RHE are reported. Diffusion tests on RHE confirm the results previously obtained with human skin explants. The results on transepithelial electrical resistance (TEER) measurements support the previous observations on the transient nature of the plasma effect and the possibility to control its duration. Finally, the positive results achieved with the PTA open new possibilities for the treatment of larger surfaces up to potentially the complete human body.

## 2. Materials & methods

### 2.1. Reconstructed human epidermis (RHE)

RHEs were prepared according to the classical protocol of Frankart et al. [24], with slight modifications. Primary Normal Human Epidermal Keratinocytes (NHEKneo Lonza Bioscience, Basel, Switzerland, ref. 00192907) were defrosted and cultured in T-75 cell culture flasks in Dermalife K complete medium (CellSystems®, Kirkland, WA, USA, ref. LM-0027) with 1 % Penicillin/Streptomycin (Sigma-Aldrich, Saint-Quentin-Fallavier, France ref. P4333) for a few days until confluence. Media were changed every other day. NHEK cells were then washed with PBS (DPBS 10 $\times$  Gibco™, ThermoFisher Scientific, Illkirch-Graffenstaden, ref. 14200083) diluted at 1 $\times$  in Apyrogenic sterile water (OTEC, Laboratoire Aguetan ref. 69600018) and detached with trypsin (Trypsin/EDTA Lonza Bioscience, ref. CC-5012), centrifuged and seeded in Millicell cell culture inserts (12 mm, polycarbonate, 0.4  $\mu\text{m}$  Sigma ref. Z353078). Each insert contained a 500  $\mu\text{L}$  suspension of 400,000 cells. The inserts were placed in the center of wells from 6-well plates containing, each, 2 mL of Dermalife K and RHE culture is initiated as sketched in Schematic 1. In the proliferation phase, the plates were incubated at 37 °C with 5 % CO<sub>2</sub>, for three days. Then the media was carefully removed from the inserts to expose the cells to the air (air-liquid interface exposure) and the medium from the wells was changed to EpiLife™ medium with 60  $\mu\text{M}$  calcium (Gibco™, ThermoFisher Scientific, ref. MEPI500CA) supplemented with human keratinocyte growth supplement (Gibco™, ThermoFisher Scientific, ref. S0015), CaCl<sub>2</sub> 1.5 mM (Sigma-Aldrich) and Penicillin/Streptomycin 1 %. Vitamin C 92  $\mu\text{g}/\text{mL}$  (Sigma-Aldrich) and keratinocyte growth factor 10 ng/mL (Sigma-Aldrich ref. K1757-10UG) were added in the media. Plate cover was replaced by a Breathe-easy sealing membrane. Media were changed each 2 days for 2 weeks; this is the differentiation phase. After two weeks, reconstructed human epidermis were formed in the inserts and ready for experiments.

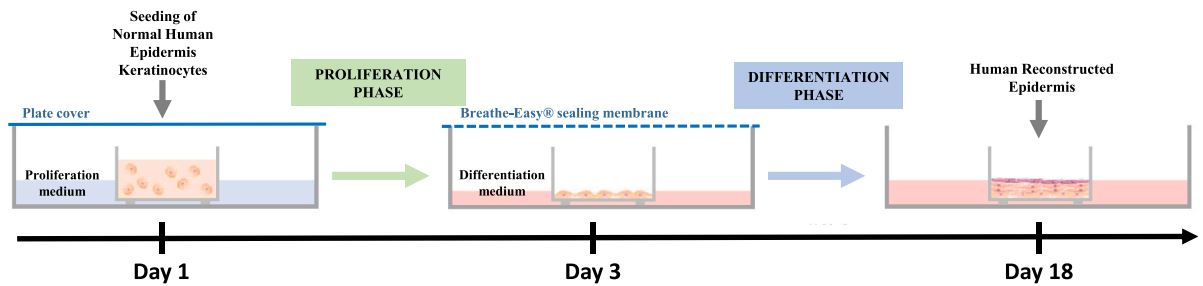
### 2.2. Reconstructed human epidermis histological analysis

Control and plasma exposed RHEs were separated from the inserts manually with a scalpel, cut in two halves and frozen following a standard snap-freezing method in OCT (Sigma-Aldrich). RHE sections, 10  $\mu\text{m}$  thick, were then cut using a Cryostat apparatus (Leica, Wetzlar, Germany). Sections were stained using a classical hematoxylin and eosin staining protocol with a hydration/rehydration step.

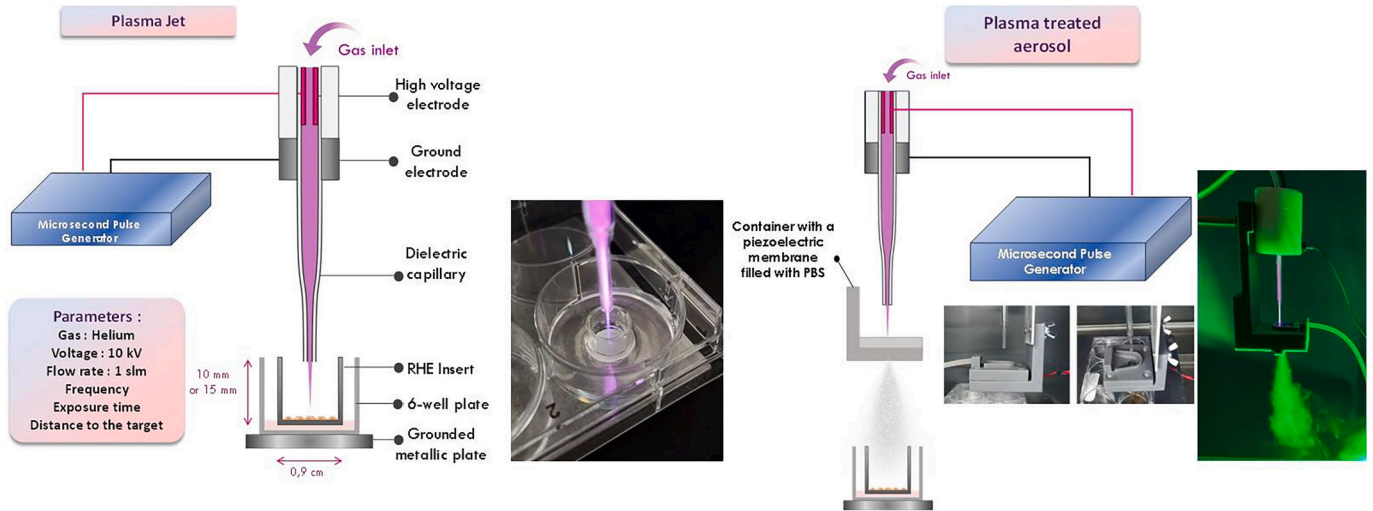
### 2.3. Plasma jet and plasma treated aerosol setups and treatment parameters

#### 2.3.1. Plasma jet

In this work, the “Plasma Gun”, a cold atmospheric plasma device developed at GREMI [1,9,10], was used for experiments. The system comprises of a tapered borosilicate capillary (dimensions are described in Schematic 2) flushed with 1 SLM (Standard Liter per Minute) of helium (Alphagaz 1 Air Liquide, France) controlled by a digital mass flow meter (red-y compact series, Vögtlin instruments) and equipped with a pair of electrodes in a dielectric barrier discharge configuration. The high voltage pulsed powered electrode is an inner cylindrical hollowed electrode while an outer 5 mm wide ring wrapped around the capillary served as the grounded electrode. The power supply generates a voltage pulse of 2  $\mu\text{s}$  full width at half maximum with a Gaussian shape and a peak amplitude of 10 kV. Pulses were delivered at either 100 Hz or 20 kHz frequency with a gap distance, from the capillary tip to the RHEs, of 10 mm and 15 mm, respectively. To produce plasma-treated PBS, 1 mL of the solution in a 24-well microplate was exposed to plasma at 20 kHz, at a distance of 15 mm. Treatment time for all the conditions was 1 min. The treatments were very short and the helium flow rate is moderate (1SLM) so that neither any temperature increase nor any significant



**Schematic 1.** Scheme of the formation of a reconstructed epidermis in a Millicell insert. Day 1: seeding of keratinocytes; Day 1 to Day 3: keratinocyte proliferation; Day 3: change of proliferation medium to differentiation medium and exposition of the cells to air-liquid interface; Day 3 to Day 18: keratinocyte differentiation and RHE formation.



**Schematic 2.** Plasma Jet (left) and Plasma treated aerosol (right) treatment setups.

drying or buffer liquid evaporation were measured. The temperature of RHEs was 20 °C and as RHEs stay in contact with the buffer liquid in well plate across a semipermeable membrane so that any drying is continuously compensated including during the plasma delivery. As shown in the photo in [Schematic 2](#), the plasma jet is delivered to the RHE in the touching mode, i.e. the plasma plume impinges over the RHE surface.

### 2.3.2. Plasma treated aerosol

The plasma treated aerosol setup includes the previously described Plasma Gun and a small container located 15 mm below the tip of the capillary ([Schematic 2](#)). This container is composed of a cavity with a piezoelectric membrane at the bottom for the nebulization of the plasma treated liquid. Before operation, 1 mL of PBS was introduced in the cavity for each treatment. The plasma gun is operated in this configuration for 1 min at 20 kHz pulse repetition rate, 10 kV peak voltage amplitude. Thus, during the treatments, the PBS extemporaneously treated by the plasma was sprayed during 1 min on the RHE positioned under the piezoelectric membrane.

The use of the grounded metallic plate under the target (See [Schematic 2](#)) is not mandatory for plasma generation as a ground electrode is already present inside the plasma reactor. Nevertheless, the electrical potential of the target affect the plasma characteristics. Therefore, all treatments and RONS measurements were performed with this plate to ensure to have the same potential and therefore reproducibility. Without this metallic plate, the well plates may stand on dielectric or metallic table in the different laboratories, which may influence the treatment outcomes as previously documented [25].

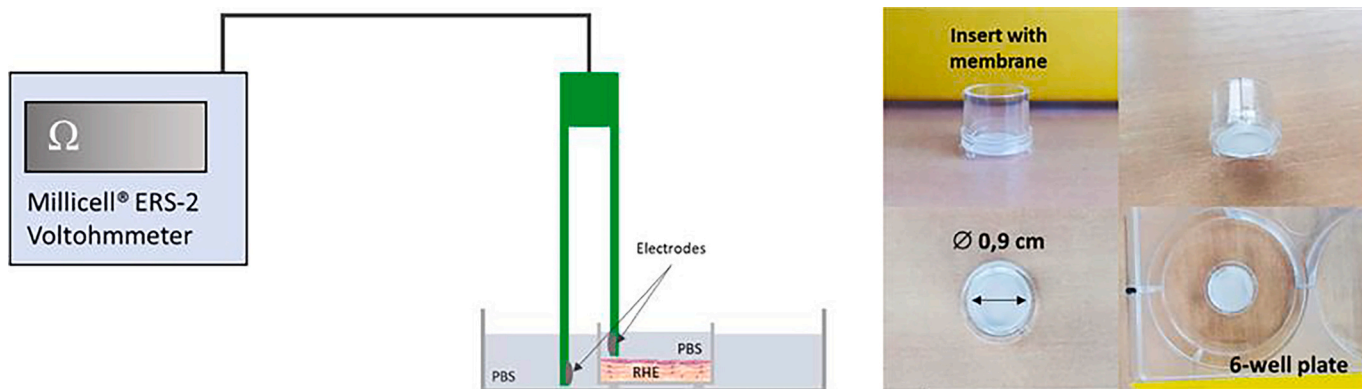
### 2.4. Transepithelial electrical resistance (TEER) measurements

TEER measurements were performed using the Millicell® ERS-2 Voltohmmeter (Merck, Darmstadt, Germany, ref. MERS00002). This device is composed of a digital reader and an electrode with two tips with silver/silver chloride (Ag/AgCl) pellet. The measurements configuration is described in [Schematic 3](#). During measurements one of the tips is immersed in the PBS inside the insert (where is the RHE) and one in the PBS outside the insert. RHEs are first treated by plasma jet or PTA without PBS on the insert. After plasma jet treatments, 500 µL of PBS is then added on the RHE in order to do the TEER measurements. During PTA treatments, both the insert with the RHE and the well containing them is sprayed over.

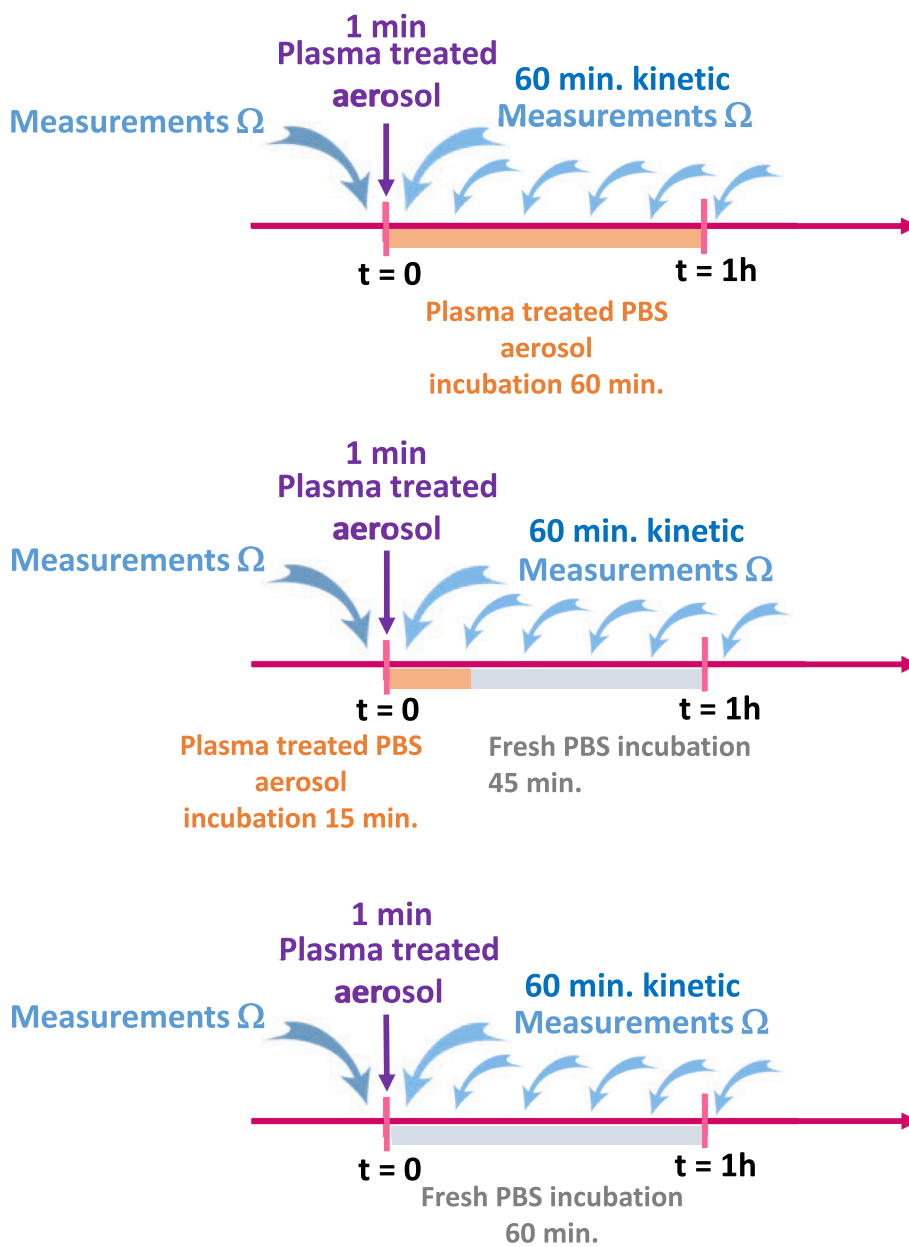
Preliminary TEER measurements were performed before plasma treatments to check the homogeneity of the RHEs. After plasma treatment the RHE resistance was collected each couple of minutes during one hour. The PBS from PTA treatment was left in contact with the RHE for different duration (60 min, 15 min or less than 10s) before being replaced with fresh PBS ([Schematic 4](#)).

### 2.5. Fluorescein permeation protocols

Permeation studies were performed using fluorescein (Sigma-Aldrich) as a fluorescent probe. The inserts containing the RHEs were placed in 6-well plates containing 2 mL of PBS and then treated by either the plasma jet or with the PTA. The fluorescein solution diluted in PBS (0.2 mg/mL) was topically applied over RHEs inside the inserts immediately after treatment. The RHEs were then incubated at 37 °C for 6 h. During this time frame, regular sampling of 100 µL of the PBS contained



Schematic 3. Schematic of TEER measurements setup and photographs of an insert from various angles and inside a 6 well plate.



Schematic 4. Plasma treated aerosol delivery and contact time protocols. TEER measurements for different contact times of the RHE with the PBS plasma treated aerosol delivered beforehand during one minute.

in the wells was done. After each sampling, 100  $\mu\text{L}$  of fresh PBS was added back in the wells. Sampling was performed every 15 min during the first hour, then every hour for 6 h. Samples were transferred to a 96-well plate and fluorescence intensity was measured using the CLARIOstar® plate reader at  $\lambda_{\text{ex}} = 488 \text{ nm}$ ,  $\lambda_{\text{em}} = 520 \text{ nm}$ .

## 2.6. RONS concentration measurement in liquid

The concentration of  $\text{H}_2\text{O}_2$  and  $\text{NO}_2^-$  in the PBS treated by the plasma gun at 20 kHz was quantified by colorimetric methods.  $\text{TiOSO}_4$  method was used for  $\text{H}_2\text{O}_2$  and Griess reagent for  $\text{NO}_2^-$ . All reagents were acquired from Sigma-Aldrich and used according to the manufacturer instructions. The absorption values were collected by mean of a microplate reader (Victor Nico by PerkinElmer).

## 2.7. Statistical analysis

Each permeation, TEER and RONS concentrations measurements experiment was performed in triplicate. All numerical data are expressed as mean  $\pm$  standard deviation. Statistical analysis was performed using GraphPad Prism or Microsoft Excel. Differences in results were considered statistically significant when  $p$  values were lower than 0.05 (\*), 0.01 (\*\*), or 0.001 (\*\*\*). Any  $p$ -value greater than 0.05 was considered statistically non-significant.

# 3. Results

## 3.1. Integrity of RHE after plasma and PTA treatments

The plasma jet operating parameters and protocol for RHE exposure were selected considering the outcomes of our previous studies. Briefly, the permeabilization of cells using plasma jet exposure at 100 Hz pulse repetition rate [9,10] and reversible permeation of skin explants using plasma jet at 1 and 20 kHz pulse repetition rate [1] were previously demonstrated. Thus, in this work the plasma jet treatment was performed at 100 Hz/10 mm gap or 20 kHz/15 mm gap. For PTA treatment the PBS was treated with the plasma gun operating at 20 kHz and 10 kV of peak voltage. The treatment time in all protocols is 1 min.

With these plasma delivery settings, in this work, the RHE structure after plasma jet and PTA treatments were assessed through epidermal staining. HE (Hematoxylin Eosin) staining provided a general overview of RHE samples' structure integrity. Fig. 1 compares two plasma jet conditions (20 kHz and 100 Hz) and one PTA condition (20 kHz) to a

control (non-treated RHE). The control (Fig. 1a) presents a normal differentiation and stratification of the epidermis with a basal layer, spiny and granular intermediate layers and a stratum corneum. Fig. 1c and d show that neither the 100 Hz plasma jet nor the 20 kHz PTA exposures for one minute reveal any RHE structure damage. Conversely, the 20 kHz plasma jet treatment (Fig. 1b) induces a slight damage on the upper layer of the RHE (stratum corneum). A localized detachment of the stratum corneum was observed. For the following experiments, these three plasma conditions were kept. As RHEs were studied only 30 min after plasma treatment in this experiment, a potential impact on cell viability would probably not have been detected. However, the exposition of Primary Normal Human Epidermal Keratinocytes (NHEK) cell in 2D culture in their culture medium to the direct plasma jet revealed no significant decrease in their viability after 24 h, being around 97 % after a one minute treatment time at 20 kHz pulse repetition rate (data not shown).

These results indicate that, while RHE is a relevant model for subsequent translation to human explants or volunteer skin exposure, it is nevertheless more sensitive than these later-stage models. It was indeed previously demonstrated that plasma jet exposure at 20 kHz repetition rate was not toxic for skin explants having a much higher thickness (ranging from 0.5 to 2 mm) than RHE. The surfaces of these targets during plasma jet exposure lead to a jet repulsion and thus to a less focused treatment resulting both in a safe and larger surface plasma treatment [1].

## 3.2. Fluorescein permeation in RHE and RONS quantification in liquid

The efficiency of plasma jet and PTA induced permeation were assessed by using fluorescein as a fluorescent probe. This probe was applied topically and the fluorescein concentration was measured by sampling the PBS solution in the underlying well. This procedure is similar to that of a diffusion cell, such as the Franz cell, system. Our results show in Fig. 2 that all plasma conditions induced an enhancement of molecular permeation across the RHE. The 100 Hz plasma jet condition appeared to be of higher efficiency than the 20 kHz plasma jet condition. Interestingly, the PTA exposure induced an efficiency similar to that of the 100 Hz plasma jet condition. These two protocols both show that the fluorescein was detected after passing through the RHE as soon as 15 min after topical application of the PBS-fluorescein solution following the 1-min plasma jet or PTA exposure. This is a much shorter time than the one hour delay measured for the control (not plasma exposed) RHE and the 20 kHz plasma groups.

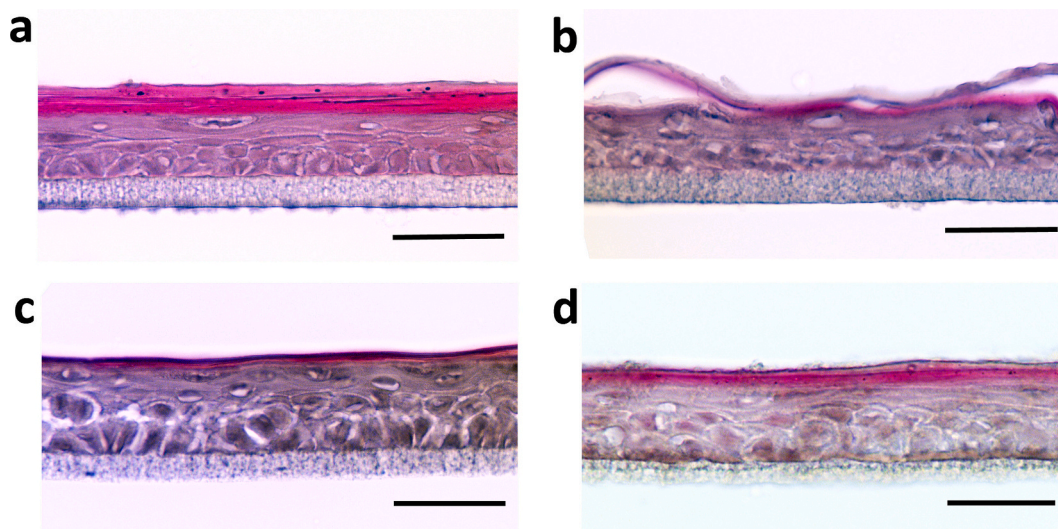


**Fig. 1.** Histological images of reconstructed human epidermis frozen sections 30 min after plasma jet and plasma treated aerosol treatments and Hematoxylin/Eosin staining. From top to bottom: a) Control, b) plasma jet 20 kHz, c) plasma jet 100 Hz, d) plasma treated aerosol. Scale bar is 50  $\mu\text{m}$ .

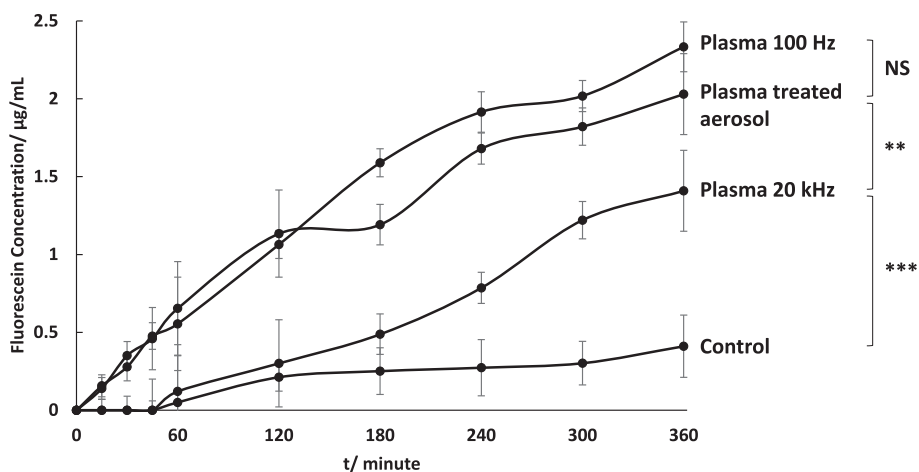


**Fig. 2.** RHE permeation kinetics of fluorescein following direct plasma jet treatments of either 20 kHz or 100 Hz and plasma treated aerosol treatments of 20 kHz. Each experiment was performed three times and each point shows the mean  $\pm$  standard deviation (statistical significance calculated for the last time point).

The plots in Fig. 2 show that the concentration of the fluorescein in the well increases quite linearly with time, revealing a linear increase of the volume of PBS-fluorescein solution transferred from the insert to the well across the RHE. Using linear fits, a rough estimation of the permeation kinetics for the different groups can be inferred. As a result, the permeation velocity is respectively of about 5; 5; 2.5 and 0.5  $\mu\text{L}/\text{h}$  for plasma jet 100 Hz, PTA, plasma jet 20 kHz and control groups, respectively. In all cases, plasma exposure results to a significant increase of the permeation kinetics. Since the PTA affects not only the RHE sample (10 mm in diameter) but also the PBS in the well containing the insert (see Fig. 3), an additional experiment was conducted to confirm that the PTA treatment specifically alters RHE permeation. This was done to ensure that the observed increase in fluorescein kinetics was not due to plasma-treated PBS in the well potentially interacting with the lower surface of the RHE. Two different 3D printed screens were used (Fig. 3): the first one with an annular shape to deliver the PTA only on the RHE and preventing it from being delivered in the well; the second one being a disk preventing the RHE exposure to PTA but keeping the PTA delivery in the well. The annular and disk shape screen images are documented on the right-hand side of Fig. 3. Furthermore, the PTA treatments were compared with a treatment by plasma-treated PBS. For this condition, 1 mL of PBS was first treated inside a 24 well microplate well with the plasma gun at 20 kHz and then applied to the RHE within few minutes.

Fig. 3 clearly demonstrates that the PTA exposure on the outside has no influence on the permeation and the results are comparable to the control group. Results from the PTA exposure only on the RHE confirm

the previously observed results. This confirms that fluorescein delivery across the RHE results from the PTA interaction with the upper surface of the RHE and is not triggered from the PTA delivered in the well. It may be possible that at least part of the observed effect on permeation is due to RONS in plasma-treated PBS. In Fig. 4, the results from the quantification of  $\text{H}_2\text{O}_2$  and  $\text{NO}_2^-$  in the PBS treated by the plasma gun (20 kHz) either in static inside the 24 well microplate or in the PTA configuration are reported. The results show higher concentrations for the static treatment compared to the PTA configuration. This observation, combined with the permeation results in Fig. 3, suggest that there is no direct correlation between long-lived RONS (i.e.  $\text{H}_2\text{O}_2$  and  $\text{NO}_2^-$ ) in the plasma treated PBS and permeation enhancement. Thus, long-lived RONS certainly do not account for the totality of the plasma effect on RHE. The higher permeation enhancement achieved by PTA, which present lower long lived RONS concentrations, supports the hypothesis that short lived reactive species and ions may play a significant role in epidermis permeation.

Our previous work on plasma jet exposure of human explants demonstrated a transient modulation of the skin barrier revealing a time window after plasma treatment of about 20 min. In this previous study, if the solutions containing cosmetic ingredients (caffeine or hyaluronic acid) were topically applied later than this time window, the permeation was not achieved. Similarly, in this work the permeation kinetics when fluorescein was applied right after the plasma treatment ( $t = 0$ ) or with a delay of 60 min were investigated. The results (Fig. 5) indicate that plasma exposure of the RHE, either with the plasma jet or with the PTA,

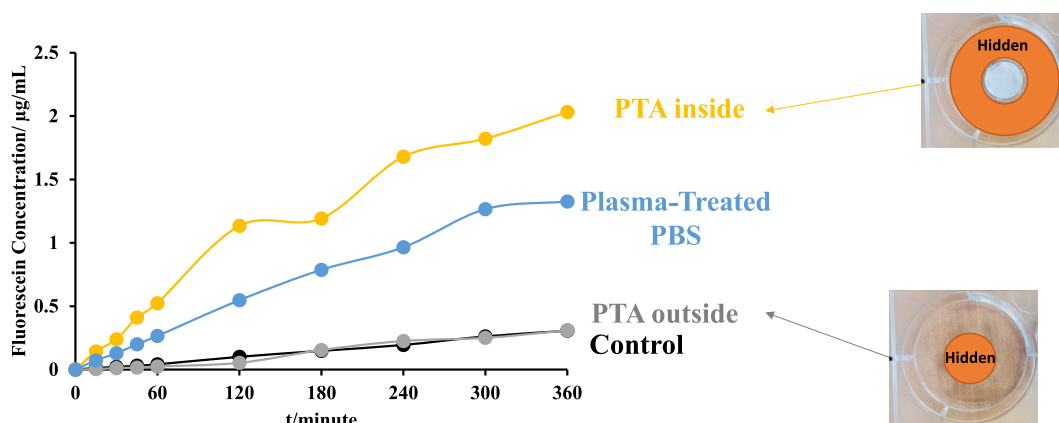


**Fig. 3.** RHE permeation kinetics of fluorescein following 20 kHz plasma treated aerosol exposures with the disk screen for “PTA outside” plot, with the annular screen for “PTA inside” plot, following addition of plasma-treated PBS and for the control condition (no plasma).

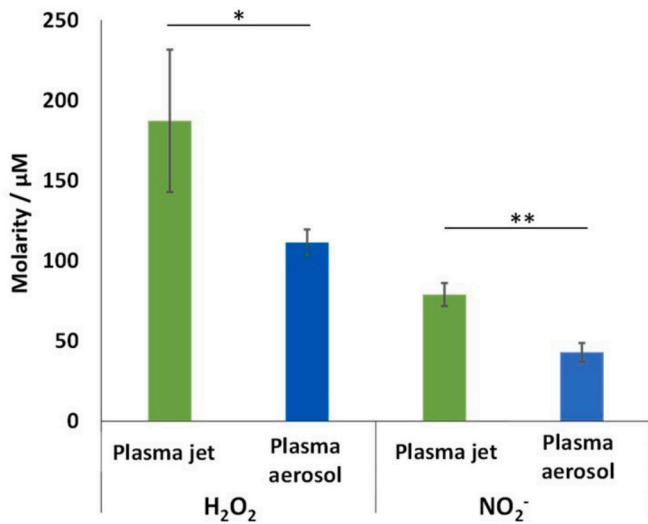


Fig. 4.  $\text{H}_2\text{O}_2$  and  $\text{NO}_2^-$  concentrations in PBS treated by plasma gun (20 kHz) in static treatment or plasma treated aerosol configuration with a treatment time of 1 min. Each experiment was performed three times and each bar shows the mean  $\pm$  standard deviation. Differences in results were considered statistically significant when  $p$  values were lower than 0.05 (\*), 0.01 (\*\*), or 0.001 (\*\*\*)

results in a time window during which permeation can be enhanced. After a 60-min long delay after plasma jet exposure, the fluorescein permeation kinetics is much slower than that measured if the fluorescein solution is applied right after plasma treatments. For PTA exposure, the right after or one-hour delay before fluorescein applications does not evidence any difference in the permeation kinetics. This is likely due to the used protocol as the PBS was plasma treated for one minute but kept in contact with the RHE during one hour before fluorescein applications. This demonstrates the non-destructive and transient nature of plasma exposure for RHE and indicates that RHE are a relevant in vitro model mimicking explant features following plasma exposure for permeation studies.

### 3.3. TEER measurements in RHE

As the accelerated penetration of fluorescein was measured, the transepithelial electrical resistance of plasma treated RHE was studied in more detail. Fig. 6 documents the measurement of TEER in control, plasma jet 100 Hz, plasma jet 20 kHz and PTA 20 kHz groups during one hour following plasma delivery. All data have been normalized to the TEER value of the RHE at the beginning of the recording for the control group and one minute before plasma delivery for all other groups. The normalization was processed to compensate the variation of the TEER value from one sample to another as all RHEs are not perfectly identical. The measurements were performed in triplicate on a different RHE for each replicate.

The control group measurements validate that the TEER value is about constant during one hour with maximum deviation of 2 %. The plasma jet exposures reveal an instantaneous but transient (3 and 25 min-long) lowering of the TEER at 100 Hz and 20 kHz respectively. The 3-min long period for the 100 Hz pulse repetition rate setting defines the time window during which the TEER decreases by about 7 % and quickly increases back to the baseline level. The 25 min-long period for the 20 kHz pulse repetition rate setting defines the time window during which the TEER is first decreased by about 7 % and then gradually recovers its initial value. The PTA exposure also results in an instantaneous lowering of the TEER value with a 15 % amplitude decrease and a subsequent slow recovering to baseline value over 60 min.

While plasma jet deliveries are limited to the RHE upper surface

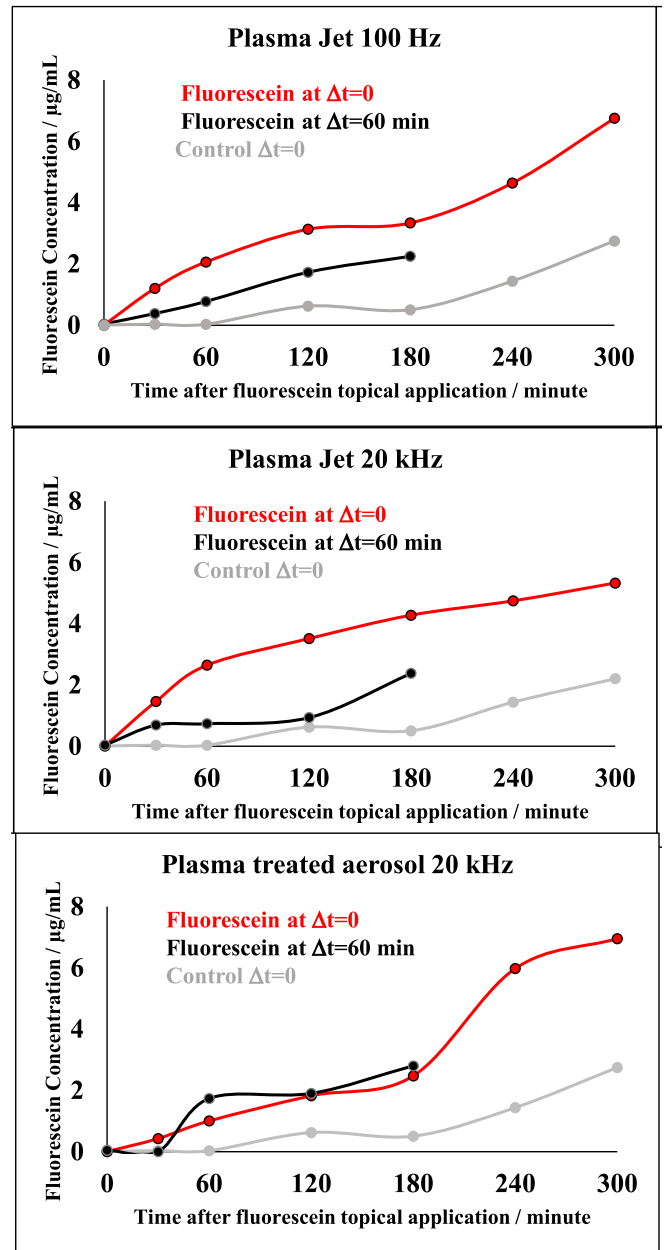


Fig. 5. RHE permeation kinetics following direct plasma jet treatments at either 100 Hz or 20 kHz and plasma treated aerosol exposure. Fluorescein was topically added right after ( $\Delta t = 0$ ) plasma jet or PTA treatments or after a 60 min delay ( $\Delta t = 60$  min).

exposure during one minute, the PTA exposure results in the covering and subsequent incubation of a PBS plasma activated liquid layer over the RHE samples.

The Fig. 7 presents the influence of PTA incubation time on RHE permeation following the protocol illustrated in Schematic 4. It is clearly observed that as soon as the PTA is removed, the TEER quickly recovers to the baseline level. The TEER decrease amplitude and kinetics appears more stochastic, maybe in coincidence with the variability of the RHE samples, being instantaneous or lasting during few minutes in different experiences. The same holds true for the amplitude of the TEER drop, ranging from about 5 to 15 %.

## 4. Discussion

In this work, reconstructed human epidermis (RHE) have been

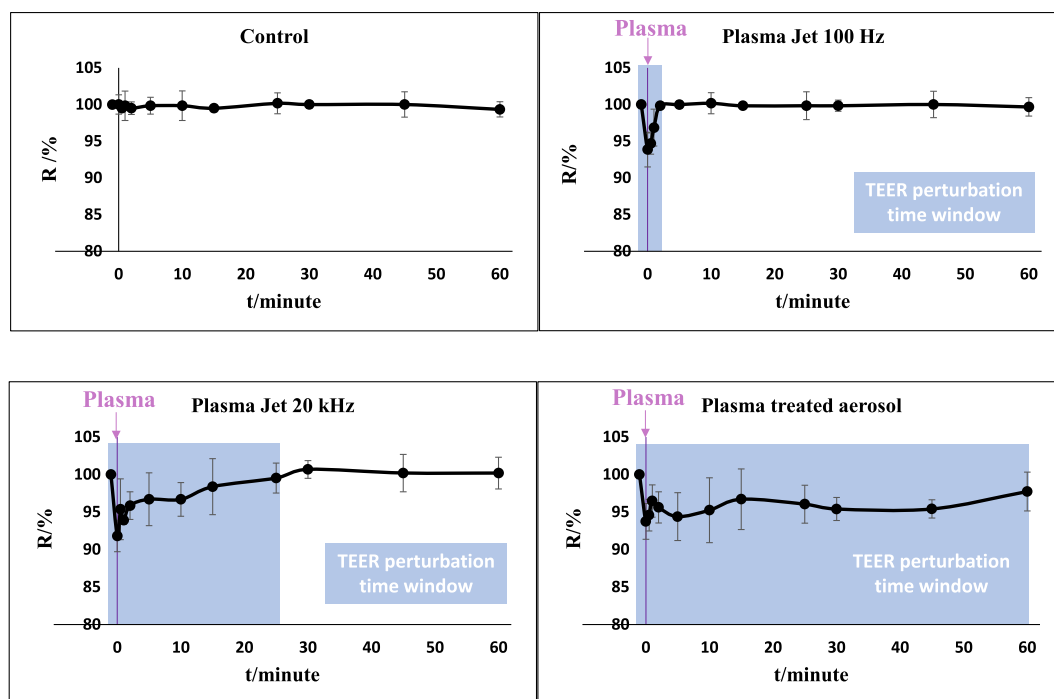


**Fig. 6.** Normalized TEER (R) measurements for the control group (no plasma exposure), after plasma jet treatment at 100 Hz, plasma jet treatment at 20 kHz, plasma treated aerosol exposure. The vertical pink line indicate the time of plasma delivery. The rectangles illustrate the time window during which the TEER value is changed before recovering the initial value. (For interpretation of the references to colour in this figure legend, the reader is referred to the web version of this article.)

cultured and used as a 3D *in vitro* model to study their relevance as skin surrogates for CAP technology implementation in future skin care or skin treatment applications. The RHE have been exposed to CAP to study plasma-assisted permeation in 3D *in vitro* models in the perspective of developing plasma-based protocols for dermatology, cosmetics, and any other plasma medicine applications where skin is the first barrier to access organs, tumors, tissue. Both helium plasma jets and plasma treated PBS aerosols have been employed to treat RHE, evaluating their permeation-enhancing capabilities and elucidating their mechanisms of action for transdermal delivery. Histological analysis confirms that moderate peak voltage amplitude (10 kV in this work), short time exposures (one minute in this work), gap distance of about 10 mm and pulse repetition rate up to 20 kHz is safe and non-toxic for RHE exposure, in line with previous demonstration for cell culture and human explants. Histological analysis confirm that treatment protocols (1 min of exposure at 10 kV, 100 Hz-20 kHz, 10 mm gap) previously demonstrated safe on cell culture, pig skin and human explants [1,9,10] were also safe and non-toxic for RHE.

To the best of our knowledge, this work is the first demonstration of RHE permeation enhancement not only with plasma jet exposure but with plasma treated aerosol as well. Toxicity and permeation studies indicate that RHE is a relevant *in vitro* model to study plasma exposure, being safe and confirming previous demonstration on the possibility to achieve transient and reversible skin barrier permeation. The transient nature of plasma jet and plasma treated aerosol assisted permeation documented in Fig. 5 showing that if the fluorescein enriched PBS solution is topically applied with a 60 min delay after plasma jet or plasma treated aerosol exposure, the permeation kinetics is slowed down. This confirms, in line with previous plasma jet exposure of human explants, that plasma action is transient and safe considering histological analysis (Fig. 1).

The plasma impact on skin barrier was assessed by measuring the TEER resistance of RHEs. Plasma jet exposure lead to instantaneous decrease of TEER and either quick (100 Hz setting) or longer (20 kHz setting) recovering of TEER (Fig. 6). Plasma treated aerosol also lead to

TEER decrease but with a much longer persisting period if plasma sprayed solution is kept in contact with the RHE. Conversely, if the plasma sprayed solution is washed at some delay, the TEER resistance quickly recovers to the baseline level (Fig. 7).

While demonstrating the efficient and transient nature of RHE modulation following plasma jet or plasma treated aerosol exposure, more work is still needed to correlate the RHE resistance features with the permeation efficiency with different plasma delivery protocols. Nevertheless, the plasma treated aerosol and plasma jet exposures reported in this work allow initiating the discussion on the mode of action for plasma-assisted permeation:

The plasma jet treatment not only consists in the exposure to reactive species but also during the treatment course to intense transient electric fields delivered at each plasma pulse. Cell membrane electroporation and combination of this physical process with the availability of plasma-derived reactive species, both short and long living, renders the direct plasma jet treatment different from that of the plasma-activated aerosol. Such combined physicochemical mode of action was indeed reported in few studies based on the use of pulsed electric field and plasma activated solution exposure [11,26]. Besides this difference, the mechanism of interaction of plasma treated aerosol or plasma jet generated reactive species with cell membrane on the molecular level implies both redox and phosphorylation signaling with proteins [27]. Besides signaling action, reactive nitrogen and oxygen species initiate lipid peroxidation. It was demonstrated that the conjugate role of peroxynitrite, peroxynitrous acid (ONOOH), and/or its decomposition products, i.e., OH and nitrogen dioxide (NO<sub>2</sub>), initiate lipid peroxidation [28]. Peroxynitrite resulting from the diffusion-controlled reaction between nitric oxide and superoxide anion radical, reacts with lipids, DNA, and proteins via direct oxidative reactions or via indirect, radical-mediated mechanisms. These reactions trigger cellular responses ranging from subtle modulations of cell signaling to overwhelming oxidative injury, committing cells to necrosis or apoptosis [29]. More details on the mode of action of electric field, electrical current and reactive species in cell permeabilization and on stratum corneum loosening can be found in the recent review paper

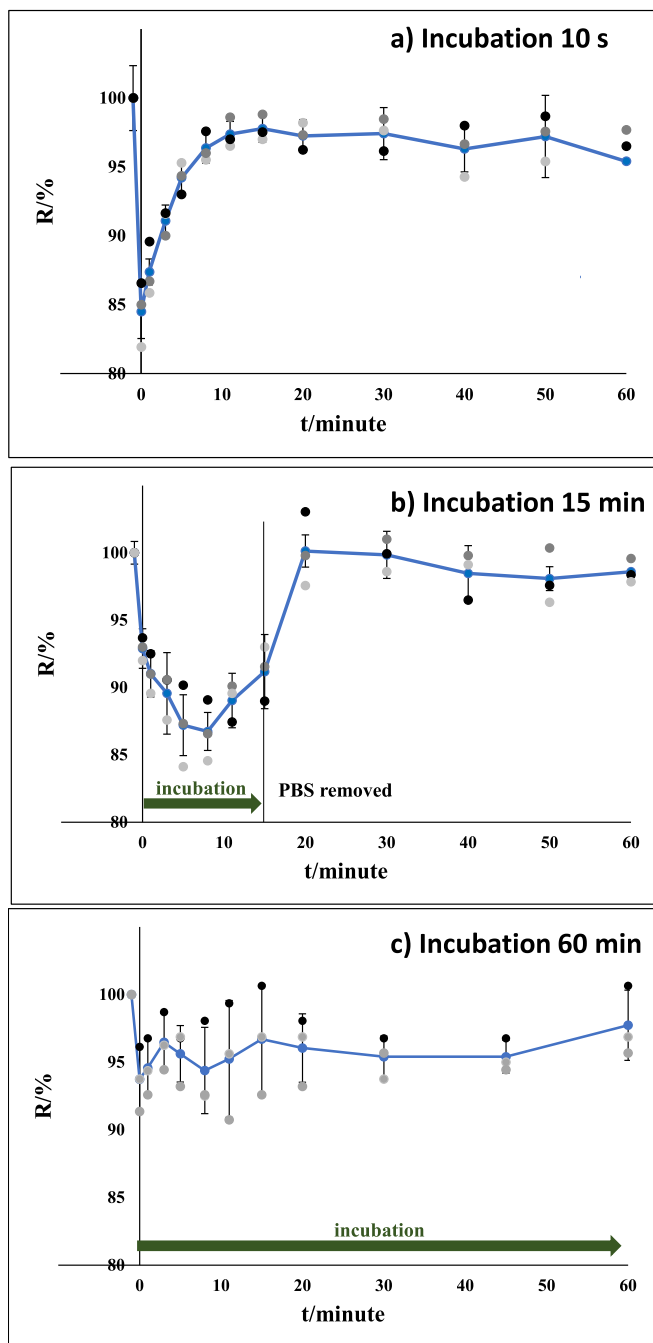


**Fig. 7.** Normalized TEER measurements after plasma treated aerosol exposure and incubation (green arrow) with sprayed plasma-treated PBS for (a) 10 s, (b) 15 min, (c) 60 min. (For interpretation of the references to colour in this figure legend, the reader is referred to the web version of this article.)

by Kristof et al. [30].

The plasma treated aerosol induced permeation cannot be caused by the electrical current delivered by the plasma jet. The role of electric field is also discarded, as RHE are exposed several centimeter away from the plasma jet treating the PBS solution. The electric field amplitude on RHE samples is thus extremely reduced during PTA exposure [31]. Therefore, the plasma treated aerosol effect on the skin barrier is likely due to other components transported by the liquid phase and delivered in form of droplets over the RHE. This was confirmed first, in Fig. 3 as the permeation measured by exposure to only plasma treated PBS reported an increase of the permeation and second, in Fig. 7 where the TEER resistance quickly recovers to the baseline level when the PTA

solution is removed. Anyway, the measurement of long-lived RONS in the liquid (Fig. 4) and the permeation test (Fig. 3) provide further insight. The plasma treated PBS, that present higher concentration of long-lived RONS, produced a lower increase in permeation compared to the plasma treated aerosol exposure. Thus, the plasma treated droplet have properties (other than high long-lived RONS concentrations) that are capable of inducing enhanced permeation on RHE. In the experiments illustrated in Fig. 2 and Fig. 5, the 100 Hz plasma jet protocol was shown to be more efficient for fluorescein permeation than the 20 kHz one. The increase of the pulse repetition rate leads to the exposure of the biological sample to a transient flux of short-living species at each plasma pulse during the treatment course. The demonstration of the specific role of these short-living species is not straightforward in plasma biomedical applications. Conversely, reconstructed chemical solutions having the same long-living species concentration as those generated by the plasma jet exposure can be used to assess the specific role of these stable species in the biological response. This was not performed in this study but can be envisioned in a future work. The mild detachment of the stratum corneum induced by the 20 kHz condition (Fig. 1b) may imply that other effects (e.g. localized thermal effect) are taking place during the treatment and may contrast with the permeabilization effect. Another hypothesis to explain plasma jet induced permeation would be to consider short living species delivered during the plasma jet exposure. These short living species may be partly quenched in the high pulse repetition rate regime of the plasma jet. As the time between two pulses decreases and the steady state RONS concentration increases in the 20 kHz regime, the short living species may indeed be partly quenched through the very rich plasma kinetic pathways. The investigation and check of this hypothesis would require a large experimental and modeling work, which is out of the scope of this preliminary investigation. The TEER modulation measured with plasma jet protocols is also likely partly linked with the RONS action.

The comparative analysis of TEER and permeation features following plasma jet or plasma treated aerosol exposures finally reveals the likely combined implication of RONS, short and long-living, and electrical components when these later are present during RHE treatment. Future investigations should imply larger number of RHE exposure with the different plasma jet and plasma treated aerosol protocols to deepen the understanding of the mode of action of plasma assisted skin permeation. In this perspective, the topical application of fluorescein, but also other molecules, at specific timing, in coincidence with the TEER modulation dynamics could bring precious insights. The demonstration for plasma treated aerosol induced permeation opens up exciting perspectives in the translation of this work outcomes to in vivo and clinical studies with human explants or patients. Plasma treated aerosol delivery can indeed be more easily implemented, less toxic and allow large skin surface exposure. Plasma treated aerosol efficiency may be optimized first by varying the operative condition for their generation and delivery. Different liquid solution having different properties (hydrophilic, lipophilic, amphiphilic) can be treated and nebulized to favor the interaction with skin surface. Plasma treatment and nebulization of solution encapsulating dedicated active substance for specific skin care can also be studied. The use of advanced nebulizers, and not the basic piezoelectric membrane used in this preliminary work, allow controlling the droplet size distribution together with the delivery surface size. The control of the distance between the nebulizer outlet and the skin surface is a parameter worth of investigation as the balance between the short-living and long-living species present in the droplets may be finely tuned for specific application. Finally, combined plasma treatment, consisting in a very short (second long) plasma jet or dielectric barrier discharge exposure and a subsequent plasma treated aerosol delivery may be an innovative and efficient approach to enhance transdermal delivery. It was indeed shown [1] that extremely short non-thermal plasma exposure is efficient to modulate skin hydrophilicity while preventing for any side effect (temperature increase, acidification). This first step plasma exposure will then likely favor the penetration of plasma treated aerosol

in a second step.

The transient nature of plasma jet or plasma treated aerosol on skin models is a critical outcome of this work. As skin features (pH, trans-epidermal water loss, water contact angle) are fully recovered few minutes after the plasma treatment, this indicates the non-toxic nature of non-thermal plasma treatments and represents a good indication for a safe translation to clinics. Skin barrier function is disturbed for a few couple of minutes, during which pathogen invasion can be envisioned. Nevertheless, non-thermal plasma have potent disinfection properties, demonstrated following short-term exposure and on plenty of bacteria, fungi, yeast including resistant strains [32]. The short-term application of non-thermal plasma treatment is also a good indication to speculate for a minor if not any side effect on the skin microbiome. The scale up of both the plasma jet and plasma treated aerosol technologies are under development for skin and agricultural applications. The use of multi jets and scanning protocols was demonstrated to be efficient for large surface decontamination [32] while the use of multiple nebulizers to deliver plasma treated aerosol on large surface is straightforward.

## 5. Conclusion

This work demonstrates the safe exposure and transient permeation of reconstructed human epidermis. Efficient and controlled permeation is achieved not only with helium plasma jet treatment but also, for the first time to our knowledge, with a plasma treated aerosol exposure. Both minute-long plasma jet and plasma treated aerosol exposures show no toxic effect on reconstructed epidermis, with the exception of a slight detachment of the stratum corneum layer following plasma jet treatment in the high frequency regime (20 kHz in this work). Transient permeation of fluorescein in PBS solution is demonstrated by adjusting the delay between the plasma jet or plasma treated aerosol exposures and the solution topical application. The transepithelial resistance of reconstructed human epidermis experiences also show a transient decrease following plasma jet or plasma treated aerosol exposure. The duration of reconstructed epidermis incubation with the plasma-treated aerosol determines how long the transepithelial resistance remains reduced.

Permeation of reconstructed epidermis is measured following the same duration (one-minute long) but either low frequency (100 Hz) or high frequency (20 kHz) plasma jet or plasma treated aerosol or plasma treated PBS exposure. Low frequency plasma jet and plasma treated aerosol exposures demonstrate about the same permeation efficiency higher than that achieved with the high frequency plasma jet or with the plasma treated solution treatments, these later having about the same performance. The plasma-treated aerosol demonstrates effective permeation of epidermis despite generating the lowest concentration of long-lived reactive oxygen and nitrogen species among the cases considered. This suggests that not only the concentration, but also the nature (short- vs. long-lived) and the delivery dynamics of the reactive species are likely key factors in optimizing the permeation process. Plasma treated aerosol are expected to allow for long but also short living species delivery, in comparison with the long-living only exposure with the plasma treated solution. Plasma jet exposure not only consists in long-living species exposure, but in the combined delivery of short living and electric field exposure at each plasma pulse. This work highlights the advantages of plasma-treated aerosol in the fine control of skin permeation and suggests its potential applications to clinics for efficient topical drug/cosmetic delivery.

## CRedit authorship contribution statement

**Vinodini Vijayarangan:** Writing – review & editing, Writing – original draft, Methodology, Investigation, Formal analysis, Data curation, Conceptualization. **Zeineb Maaroufi:** Methodology, Investigation. **Amaury Rouillard:** Methodology. **Septuce Gaetan-Zin:** Investigation. **Sébastien Dozias:** Methodology. **Pablo Escot-Bocanegra:** Supervision,

Funding acquisition. **Augusto Stancampiano:** Writing – review & editing, Supervision, Methodology, Investigation, Funding acquisition, Conceptualization. **Catherine Grillon:** Writing – review & editing, Supervision, Project administration, Funding acquisition, Conceptualization. **Eric Robert:** Writing – review & editing, Supervision, Project administration, Funding acquisition, Conceptualization.

## Declaration of competing interest

The authors declare that they have no known competing financial interests or personal relationships that could have appeared to influence the work reported in this paper.

## Acknowledgements

This work was supported by the ARD COSMETOSCIENCES MINIONS, the ANR-23-04CE-0003 “PLASMASOL”, the 80 Prime by CNRS for supporting Amaury Rouillard, the CNES and the University of Orléans for supporting Septuce Gaetan-Zin.

The authors thank the MO2VING-P@CYFIC facility (CBM, Orléans, France) for the acquisition of microscopy images.

## Data availability

Data will be made available on request.

## References

- [1] V. Vijayarangan, S. Dozias, C. Heusele, O. Jeanneton, C. Nizard, C. Pichon, J.-M. Pouvesle, A. Stancampiano, E. Robert, Boost of cosmetic active ingredient penetration triggered and controlled by the delivery of kHz plasma jet on human skin explants, *Front. Phys.* 11 (2023) 1173349, <https://doi.org/10.3389/fphy.2023.1173349>.
- [2] D. Athanasopoulos, P. Svarnas, S. Ladas, S. Kennou, P. Koutsoukos, On the wetting properties of human stratum corneum epidermidis surface exposed to cold atmospheric-pressure pulsed plasma, *Appl. Phys. Lett.* 112 (21) (2018), <https://doi.org/10.1063/1.5027901>.
- [3] A.T. Khalaf, A.N. Abdalla, K. Ren, X. Liu, Cold atmospheric plasma (CAP): a revolutionary approach in dermatology and skincare, *Eur. J. Med. Res.* 29 (1) (2024), <https://doi.org/10.1186/s40001-024-02088-9>.
- [4] G. Busco, E. Robert, N. Chettouh-Hammas, J.-M. Pouvesle, C. Grillon, The emerging potential of cold atmospheric plasma in skin biology, *Free Radic. Biol. Med.* 161 (2020) 290–304, <https://doi.org/10.1016/j.freeradbiomed.2020.10.004>.
- [5] F. Tan, Y. Wang, S. Zhang, R. Shui, J. Chen, Plasma dermatology: skin therapy using cold atmospheric plasma, *Front. Oncol.* 12 (2022), <https://doi.org/10.3389/fonc.2022.918484>.
- [6] S. Bekeschus, D. Singer, G. Ratnayake, K. Ruhnau, K. Ostrikov, E.W. Thompson, Rationales of cold plasma jet therapy in skin cancer, *Exp. Dermatol.* 34 (2) (2025), <https://doi.org/10.1111/exd.70063>.
- [7] A. Kazemi, M.J. Nicol, S.G. Bilén, G.S. Kirimanjeswara, S.D. Knecht, Cold atmospheric plasma medicine: applications, challenges, and opportunities for predictive control, *Plasma* 7 (1) (2024) 233–257, <https://doi.org/10.3390/plasma7010014>.
- [8] C.Y. Koga-Ito, K.G. Kostov, F.S. Miranda, N.V.M. Milhan, N.F. Azevedo Neto, F. Nascimento, R.S. Pessoa, Cold atmospheric plasma as a therapeutic tool in medicine and dentistry, *Plasma Chem. Plasma Process.* 44 (3) (2023) 1393–1429, <https://doi.org/10.1007/s11090-023-10380-5>.
- [9] V. Vijayarangan, A. Delalande, S. Dozias, J.-M. Pouvesle, C. Pichon, E. Robert, Cold atmospheric plasma parameters investigation for efficient drug delivery in HeLa cells, *IEEE Trans. Radiat. Plasma Med. Sci.* 2 (2) (2017) 109–115, <https://doi.org/10.1109/trpms.2017.2759322>.
- [10] V. Vijayarangan, A. Delalande, S. Dozias, J.-M. Pouvesle, E. Robert, C. Pichon, New insights on molecular internalization and drug delivery following plasma jet exposures, *Int. J. Pharm.* 589 (2020) 119874, <https://doi.org/10.1016/j.ijpharm.2020.119874>.
- [11] T.H. Chung, A. Stancampiano, K. Sklias, K. Gazeli, F.M. André, S. Dozias, C. Douat, J.-M. Pouvesle, J.S. Sousa, E. Robert, L.M. Mir, Cell electroporation enhancement by non-thermal-plasma-treated PBS, *Cancers* 12 (1) (2020), <https://doi.org/10.3390/cancers12010219>.
- [12] S. Sasaki, R. Honda, Y. Hokari, K. Takashima, M. Kanzaki, T. Kaneko, Characterization of plasma-induced cell membrane permeabilization: focus on oh radical distribution, *J. Phys. D: Appl. Phys.* 49 (33) (2016) 334002, <https://doi.org/10.1088/0022-3727/49/33/334002>.
- [13] P.R. Sreedevi, K. Suresh, K., Cold atmospheric plasma mediated cell membrane permeation and gene delivery-empirical interventions and pertinence, *Adv. Colloid Interf. Sci.* 320 (2023) 102989, <https://doi.org/10.1016/j.cis.2023.102989>.

- [14] M. Gelker, C.C. Müller-Goymann, W. Viöl, Plasma permeabilization of human excised full-thickness skin by mS- and nS-pulsed DBD, *Skin Pharmacol. Physiol.* 33 (2) (2020) 69–76, <https://doi.org/10.1159/000505195>.
- [15] G. Daeschlein, S. Scholz, R. Ahmed, A. Majumdar, T. von Woedtke, H. Haase, M. Niggemeier, E. Kindel, R. Brandenburg, K.D. Weltmann, M. Jünger, Cold plasma is well-tolerated and does not disturb skin barrier or reduce skin moisture, *JDDG: J. Dtsch. Dermatol. Ges.* 10 (7) (2012) 509–515, <https://doi.org/10.1111/j.1610-0387.2012.07857.x>.
- [16] R. Shakouri, M.R. Khani, S. Samsavar, M.A. Zezeh, F. Abdollahimajid, S.I. Hosseini, A. Dilmaghanian, E. Ghasemi, M.R. Alihoseini, B. Shokri, In vivo study of the effects of a portable cold plasma device and vitamin C for skin rejuvenation, *Sci. Rep.* 11 (1) (2021), <https://doi.org/10.1038/s41598-021-01341-z>.
- [17] K. Heuer, M.A. Hoffmanns, E. Demir, S. Baldus, C.M. Volkmar, M. Röhle, P. C. Fuchs, P. Awakowicz, C.V. Suschek, C. Opländer, The topical use of non-thermal dielectric barrier discharge (DBD): nitric oxide related effects on human skin, *Nitric Oxide* 44 (2015) 52–60, <https://doi.org/10.1016/j.niox.2014.11.015>.
- [18] J.W. Fluhr, S. Sassning, O. Lademann, M.E. Darvin, S. Schanzer, A. Kramer, H. Richter, W. Sterry, J. Lademann, In vivo skin treatment with tissue-tolerable plasma influences skin physiology and antioxidant profile in human stratum corneum, *Exp. Dermatol.* 21 (2) (2012) 130–134, <https://doi.org/10.1111/j.1600-0625.2011.01411.x>.
- [19] M. Gelker, C.C. Müller-Goymann, W. Viöl, Permeabilization of human stratum corneum and full-thickness skin samples by a direct dielectric barrier discharge, *Clin. Plasma Med.* 9 (January) (2018) 34–40, <https://doi.org/10.1016/j.cpm.2018.02.001>.
- [20] J.H. Choi, S.H. Nam, Y.S. Song, H.W. Lee, H.J. Lee, K. Song, J.W. Hong, G.C. Kim, Treatment with low-temperature atmospheric pressure plasma enhances cutaneous delivery of epidermal growth factor by regulating E-cadherin-mediated cell junctions, *Arch. Dermatol. Res.* 306 (2014) 635–643, <https://doi.org/10.1007/s00403-014-1463-9>.
- [21] A.S. Agonia, A.P. de Oliveira, C. Cardoso, C. Augusto, C. Pellevoisin, C. Videau, R. J. Dinis-Oliveira, R.P. de-Oliveira, Reconstructed human epidermis: an alternative approach for in vitro bioequivalence testing of topical products, *Pharmaceutics* 14 (8) (2022) 1554, <https://doi.org/10.3390/pharmaceutics14081554>.
- [22] S. Blackert, B. Haertel, K. Wende, T. von Woedtke, U. Lindequist, Influence of non-thermal atmospheric pressure plasma on cellular structures and processes in human keratinocytes (HaCaT), *J. Dermatol. Sci.* 70 (3) (2013) 173–181, <https://doi.org/10.1016/j.jdermsci.2013.01.012>.
- [23] C.S. Dejonckheere, A. Torres-Crigna, J.P. Layer, K. Layer, S. Wiegrefe, G.R. Sarria, D. Scafa, D. Koch, C. Leitzen, M.A. Köksal, T. Müdder, A. Abramian, C. Kaiser, A. Faridi, M.B. Stope, A. Mustea, F.A. Giordano, L.C. Schmeel, Non-invasive physical plasma for preventing radiation dermatitis in breast Cancer: a first-in-human feasibility study, *Pharmaceutics* 14 (9) (2022) 1767, <https://doi.org/10.3390/pharmaceutics14091767>.
- [24] A. Frankart, J. Malaisse, E. De Vuyst, F. Minner, C.L. de Rouvroit, Y. Poumay, Epidermal morphogenesis during progressive in vitro 3D reconstruction at the air-liquid interface, *Exp. Dermatol.* 21 (11) (2012) 871–875, <https://doi.org/10.1111/exd.12020>.
- [25] A. Stancampiano, T.-H. Chung, S. Dozias, J.-M. Pouvesle, L.M. Mir, E. Robert, Mimicking of human body electrical characteristic for easier translation of plasma biomedical studies to clinical applications, *IEEE Trans. Radiat. Plasma Med. Sci.* 4 (3) (2020) 335–342, <https://doi.org/10.1109/TRPMS.2019.2936667>.
- [26] R. Mentheour, Z. Machala, Coupled antibacterial effects of plasma-activated water and pulsed electric field, *Front. Phys.* 10 (2022) 895813, <https://doi.org/10.3389/fphy.2022.895813>.
- [27] A. Privat-Maldonado, A. Schmidt, A. Lin, K.D. Weltmann, K. Wende, A. Bogaerts, S. Bekeschus, ROS from physical plasmas: redox chemistry for biomedical therapy, *Oxid. Med. Cell. Longev.* (2019) 9062098, <https://doi.org/10.1155/2019/9062098>.
- [28] R. Radi, J.S. Beckman, K.M. Bush, B.A. Freeman, Peroxynitrite-induced membrane lipid peroxidation: the cytotoxic potential of superoxide and nitric oxide, *Arch. Biochem. Biophys.* 288 (1991) 481–487, [https://doi.org/10.1016/0003-9861\(91\)90224-7](https://doi.org/10.1016/0003-9861(91)90224-7).
- [29] P. Pacher, J.S. Beckman, L. Liaudet, Nitric oxide and peroxynitrite in health and disease, *Physiol. Rev.* 87 (2007) 315–424, <https://doi.org/10.1152/physrev.00029.2006>.
- [30] J. Kristof, M.G. Blajan, K. Shimizu, A review on advancements in atmospheric plasma-based decontamination and drug delivery (invited paper), *J. Electrostat.* (2025) 104083, <https://doi.org/10.1016/j.elstat.2025.104083>.
- [31] T. Darny, J.-M. Pouvesle, V. Puech, C. Douat, S. Dozias, E. Robert, Analysis of conductive target influence in plasma jet experiments through helium metastable and electric field measurements, *Plasma Sources Sci. Technol.* 26 (4) (2017) 045008, <https://doi.org/10.1088/1361-6595/aa5b15>.
- [32] T. Maho, R. Binois, F. Brulé-Morabito, M. Demasure, C. Douat, S. Dozias, P. Escot Bocanegra, I. Goard, L. Hocqueloux, C. Le Helloco, I. Orel, J.-M. Pouvesle, T. Prazuck, A. Stancampiano, C. Tocaben, E. Robert, Anti-bacterial action of plasma multi-jets in the context of chronic wound healing, *Appl. Sci.* 11 (20) (2021) 9598, <https://doi.org/10.3390/app11209598>.